

## Fluid Flow and Thermal Characteristics in a Microchannel With Cross-flow Synthetic Jet

T T Chandratilleke, D Jagannatha and R Narayanaswamy

Department of Mechanical Engineering, Curtin University  
GPO Box U 1987, Perth, Western Australia, Australia

### Abstract

This paper presents a study of fluid and thermal characteristics in a unique hybrid heat sink with application potential in high-performance microelectronic cooling. The proposed method utilises the combined flow of pulsed fluid jet acting across the flow within a micro passage in the heat sink. An oscillating diaphragm generates an air jet with zero net mass discharge through the orifice while producing high fluid momentum outflow, hence termed “synthetic jet”. The jet and micro passage flow interaction is modelled using unsteady Reynolds-averaged Navier-Stokes equations with appropriate turbulence models. The simulation obtains the time-dependant flow profiles and the heat sink thermal performance for a range of diaphragm frequency and amplitudes. The analysis accounts for air compressibility and examines the effects of cross-flow on heat sink’s performance. The results indicate that the pulsed jet mechanism generates strong vortices that periodically impinge on the heated wall with intermittent interruption to boundary layer growth. The cross-flow drag significantly alters the heat sink flow characteristics. This hybrid heat sink achieves up to 4.3-fold thermal enhancement compared to a heat sink based only on microchannel flow. The air compressibility causes the jet discharge to cease temporarily at a certain diaphragm frequency. The proposed technique has the unique ability to produce strong fluid jet impingement and intense heat dissipation without additional fluid circuits or increased pressure drop.

### Introduction

Effective cooling solutions are critical for preventing thermal breakdown of semiconductor components. High circuit density and complex functionality in modern microelectronic devices have led to dramatic increases in internal heat generation in recent years, thus creating acute cooling requirements. In the face of this, the conventional cooling methods are rapidly becoming inadequate for intense heat loads often encountered in new microprocessors. The microelectronic industry signals an urgent need to develop practical and effective cooling methods that surpass current thresholds of thermal performance. Microchannel heat sinks have become the frontier technology in this respect and show well recognised potential for meeting high heat dissipation needs.

Extensive numerical modelling and experimentation have helped better understanding of microchannel behaviour. Studies by Lee et al. [1] have shown that the conventional Navier-Stokes equations do accurately predict microchannel characteristics within 5 percent error margin. Qu and Mudawar [2] have also drawn similar conclusions on the use of conventional equations for microchannel analysis. Lee and Garimella [3] have developed a generalised correlation for both local and average Nusselt number in terms of microchannel aspect ratio in developing laminar flow, which is universally recognised for its applicability. The present work adopts a conjugate heat transfer

model for microchannel analysis in line with the current state of numerical modelling [4].

In enhancing thermal performance of microchannels, Steinke and Kandlikar [5] and Narayanaswamy et al. [6] have shown very promising prospects with internal fins as a passive option although the increased pressure drop would be a design concern. Nevertheless, active methods are envisaged to be more effective for future cooling needs, especially if the pressure drop penalties can be avoided. Such an option is discussed below.

The present study proposes a new active enhancement method for micro fluid passages using a pulsating jet, as shown in Fig. 1. This arrangement uses a high-speed fluid jet that is ejected into the micro passage during the inward motion of the oscillating diaphragm. On retreating, the diaphragm draws fluid back into the cavity. Over one diaphragm cycle, the net mass delivered through the orifice is zero although the jet discharges an intense net outflow of fluid momentum in to the microchannel. Hence, this jet is known as “synthetic jet” or Zero-Net-Mass-Flux jet.

An unsteady vortex formation is associated with the synthetic jet operation under a special parametric condition. These vortices are illustrated to be responsible for high heat transfer at a jet-impinging surface [7]. Holman et al. [8] showed that the formation is governed by the non-dimensional groups Reynolds number ( $Re$ ) and Stokes number ( $S$ ), and is given by  $Re/S^2 > K$ , where the constant  $K \approx 1$  for two-dimensional jets and 0.16 for axi-symmetric synthetic jets. This requirement has been duly considered in selecting dimensions for the proposed model.

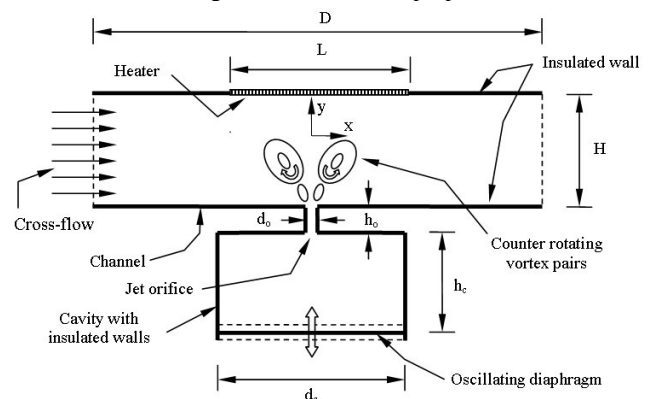


Figure 1. Schematic diagram of synthetic jet hybrid heat sink

### Model Description

The geometrical dimensions are essentially selected to comply with the synthetic jet formation requirements of  $Re/S^2 > 1$  indicated by Holman et al. [8]. The dimensions used are: orifice width  $d_o = 50 \mu\text{m}$ , orifice length  $h_o = 50 \mu\text{m}$ , channel height  $H = 500 \mu\text{m}$ , channel length  $D = 2250 \mu\text{m}$ , heater length  $L = 750 \mu\text{m}$ , cavity width  $d_c = 750 \mu\text{m}$  and cavity height  $h_c = 500 \mu\text{m}$ . The simulation is developed as a 2-dimensional model on FLUENT

using a structured mesh over the solution domain. All solid walls including the diaphragm were considered adiabatic. The heater surface was treated as isothermal at 360 K. The (left) flow inlet to the microchannel was taken as a known constant velocity boundary while a constant static pressure was applied on the (right) flow outlet. The inlet temperature of working fluid air was assumed to be 300 K with constant thermodynamic properties under standard atmospheric conditions.

A special User Defined Function (UDF) with Dynamic-layering technique was formulated to describe the periodic diaphragm movement, which is expressed as  $y = A \sin(\omega t)$ , where  $A$  is the diaphragm amplitude,  $\omega$  is the angular frequency and  $t$  is time. A segregated solution method with implicit solver formulation was used in the numerical algorithm. The Second-order discretisation schemes were employed for density, momentum, pressure, kinetic energy, specific dissipation rate and energy. The Pressure-Implicit with Splitting of Operators (PISO) scheme was used for pressure-velocity coupling. The bulk temperature of air at every time step was calculated using an UDF while the updated bulk temperature was fed back to the simulation for calculating local heat transfer coefficient and Nusselt number. The jet Reynolds number was calculated based on the jet characteristic velocity  $U_c$ , which is defined by Smith [9] as,

$$U_c = L_s f = \frac{1}{T} \int_0^{\frac{1}{2}T} u_0(t) dt \quad (1)$$

where  $u_0(t)$  is the jet velocity at the orifice discharge plane,  $\frac{1}{2}T$  is the jet discharge time or half period of diaphragm motion, and  $L_s$  is the stroke length (discharged fluid length through orifice during the upward diaphragm stroke). With these conditions, the unsteady, Reynolds-averaged Navier-Stokes equations within the solution domain were solved along with the energy equation for a range of operating conditions, which are given in Table 1.

Parameter	Range
Micro passage inlet velocity, $V_i$ (m/s)	0, 0.5, 1.0, 2.0
Diaphragm frequency, $f$ (kHz)	10
Diaphragm Amplitude, $A$ ( $\mu\text{m}$ )	0, 25, 50, 75, 100
Jet Reynolds Number, $Re$	15, 30, 46, 62
Orifice to Plate distance, $H/d_o$	10

Table 1. Parametric range for the study

The simulation was carried out for 720 time steps per cycle. At each time step, the iterations were continued until the mass, momentum and energy residuals reduced below  $10^{-6}$ , which is the convergence criterion for the computation. Data were extracted at every twentieth time step giving 36 data points per cycle. It was observed that 10 diaphragm cycles would achieve quasi-steady conditions in the flow geometry. The grid dependency was tested by noting the changes in time-averaged velocity fields for varied grid sizes. For the moving mesh integrity and CPU time, the most appropriate grid size was found to be 48072 cells for a five percent tolerance among several grid sizes. The grid density in the vicinity of the orifice was refined to have 14 grid cells in the axial direction and 20 in the transverse direction. Owing to small length scales, synthetic jets generally operate with low Reynolds numbers. However, the oscillating flow may create intense localised perturbations and wide flow variations. The Shear-Stress-Transport (SST)  $k-\omega$  turbulence model was invoked to account for the near-wall region of wall-bounded turbulent flows. Initially 3% turbulence intensity is applied at the outlets, thereafter the flow is allowed to develop on its own through the inherent instabilities. The  $y^+$  and  $y^*$  value in the wall region were found to be about 1, confirming that the near-wall mesh resolution is in the laminar sublayer. The validation of the numerical model with experimental data is presented in Chandratilleke et. al [10].

## Results and Discussion

### Velocity characteristics

Figs. 2(a) and (b) show typical time-lapsed velocity contours within the solution domain respectively for two separate cases of synthetic jet acting on stagnant fluid and flowing fluid in the micro passage. During the diaphragm upward motion, a high-velocity fluid jet is discharged through the orifice into the flow in micro passage. Determined by diaphragm amplitude, sufficiently strong jet momentum enables the jet to penetrate the micro passage flow to reach the heated (upper) wall within the time up to  $t = \frac{1}{2}T$  at the peak diaphragm displacement. In the figures, the formation of synthetic jet vortices is clearly visible during this initial phase of sequence. The flow patterns exhibits symmetry in Fig. 2 (a) while the cross-flow drag imparted by the micro passage fluid stream gives rise to asymmetry in Fig. 2 (b) where the jet is swayed in the streamwise direction. For  $t > \frac{1}{2}T$ , the diaphragm retreats from its peak displacement to complete the cycle. During this final phase, the synthetic jet mechanism draws fluid back into the cavity. Meanwhile, the synthetic jet vortices formed previously are washed downstream.

It is illustrated that the synthetic jet action periodically interrupts and breaks up the developing thermal and hydrodynamic boundary layers at the heated top wall of the micro passage. This flow interaction creates steep velocity and temperature gradients at the heated surface as long as jet impingement occurs. The pulsating jet flow mechanism therefore leads to improved thermal characteristics in the synthetic jet-mounted micro passage arrangement.

### Heat transfer characteristics

For a typical case with stagnant fluid in the micro passage, Fig. 3 shows the distribution of local Nusselt numbers over the heated wall for several time steps during one cycle. It indicates that initially, the Nusselt number remains very low for  $0 < t < \frac{1}{2}T$ . During this period, the synthetic jet vortices have yet to impinge on the heated surface, as depicted in Fig. 2(a). Therefore, the Nusselt number essentially has values similar to pure natural convection, which was estimated by a separate analysis to be about 0.2. The Nusselt number very rapidly increases to about 23 for  $t = \frac{2}{3}T$  when the vortices impinge on the heated surface, as shown in Fig. 2(a). A gentle decline in the Nusselt number is then noticed for  $t > \frac{2}{3}T$ . Thus compared to pure natural convection, the hybrid heat sink delivers over one cycle up to 120 times thermal enhancement at the heated wall.

Fig. 3 shows a typical distribution of local Nusselt numbers at the heated wall over one cycle for the case of fluid flowing in the micro passage. It is noticed that the distribution now shifted downstream and the peak value of the Nusselt number is reduced to about 13. This is because the increased micro passage flow drags the impinging jet with the flow, as depicted in Fig. 2(b). Thus, the velocity and temperature gradients at the heated wall are reduced along with the heat transfer rates.

Fig. 4 shows the thermal performance of the heat sink assisted by the synthetic jet. The datum value of 1 at zero jet Reynolds number represents the heat sink's thermal ability without the synthetic jet. It is evident that the synthetic jet acts to improve the heat sink's heat dissipation rate by about 4.3 times. This clearly highlights the excellent thermal enhancement potential with this hybrid arrangement which is achieved without additional fluid circuits or incurring extra pressure drop. A heat sink without jet assistance would require about 40 times flow velocity increase with 70 fold pressure drop rise to deliver this degree of thermal enhancement.

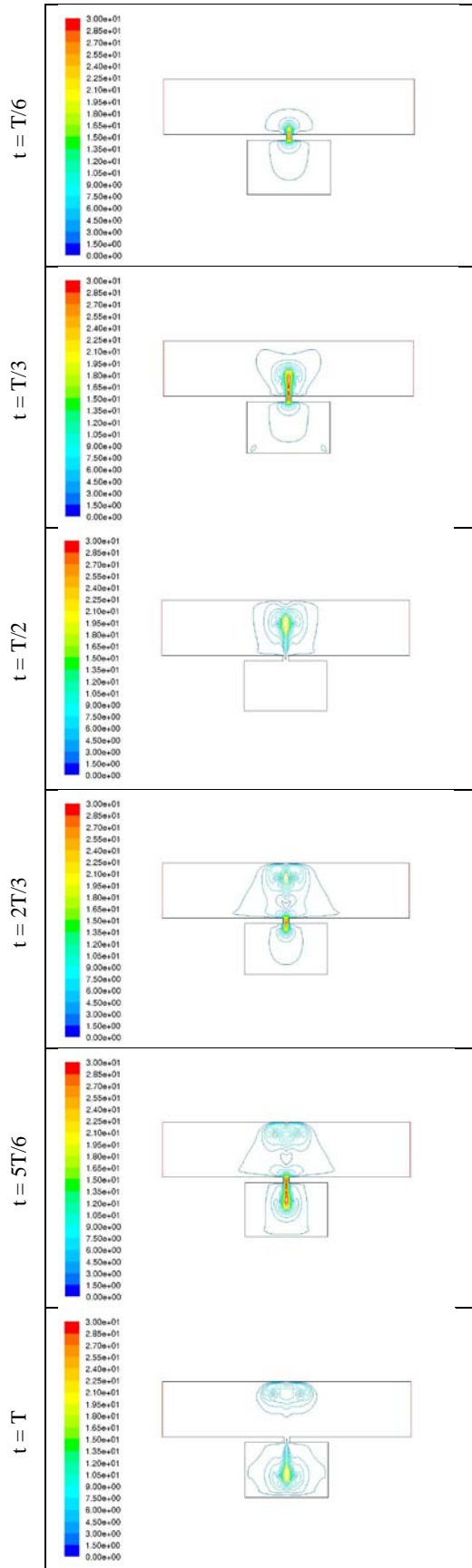


Figure 2 (a). Time-lapsed velocity contours over one diaphragm cycle  
 Micro passage velocity  $V_i = 0$  m/s,  $A = 50 \mu\text{m}$  and  $f = 10$  kHz

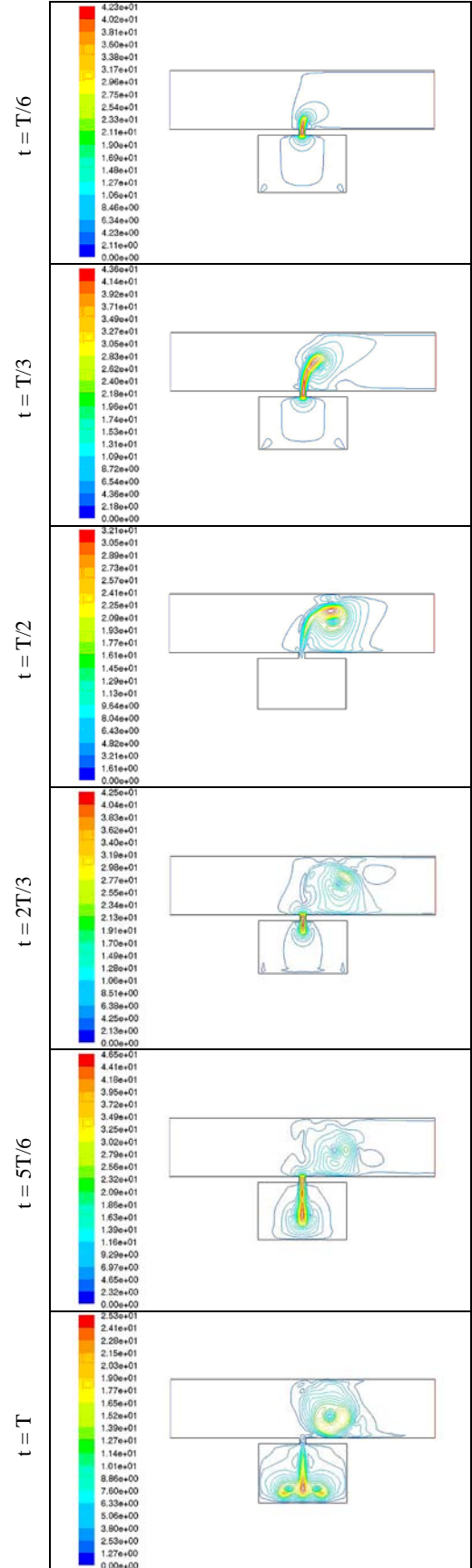


Figure 2 (b). Time-lapsed velocity contours over one diaphragm cycle  
 Micro passage velocity  $V_i = 0.5$  m/s,  $A = 50 \mu\text{m}$  and  $f = 10$  kHz

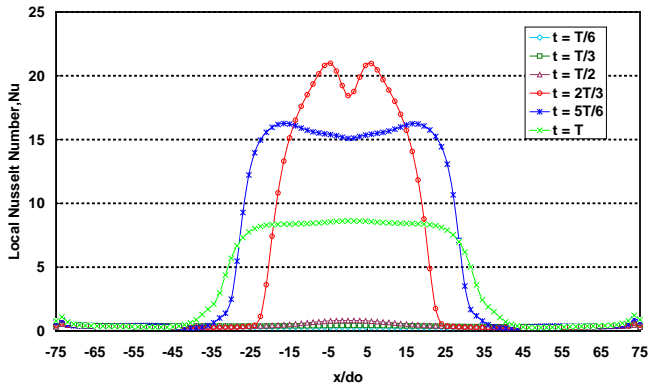


Figure 3. Distribution of local Nusselt number at the heated wall over one cycle ( $f = 10 \text{ kHz}$ ,  $A = 50 \mu\text{m}$  and  $V_i = 0 \text{ m/s}$ )

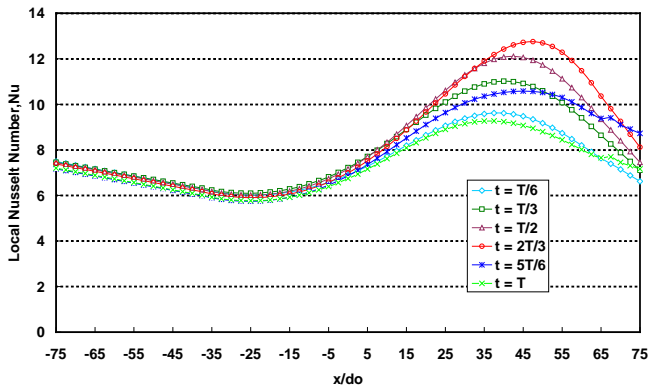


Figure 4. Distribution of local Nusselt number at the heated wall over one cycle ( $f = 10 \text{ kHz}$ ,  $A = 50 \mu\text{m}$  and  $V_i = 1 \text{ m/s}$ )

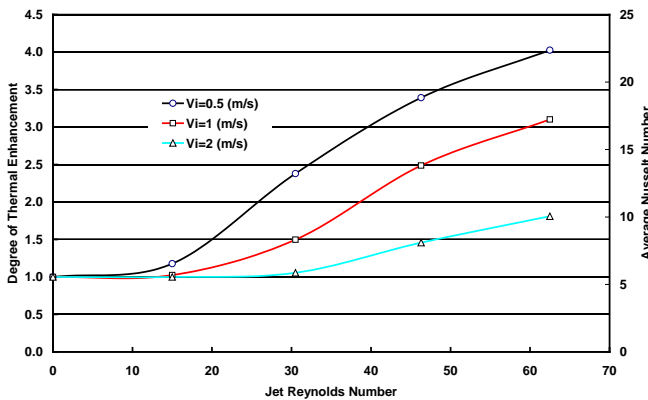


Figure 5. Thermal enhancement in synthetic jet heat sink

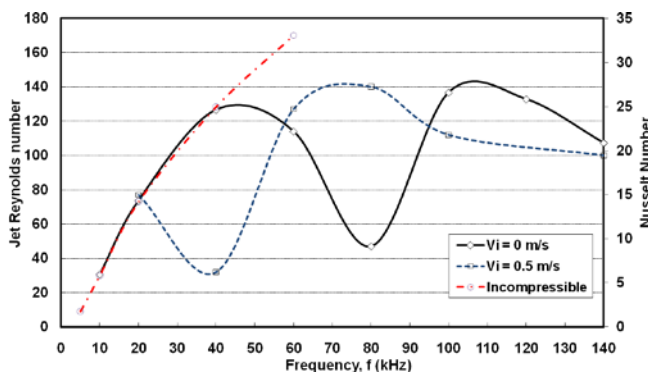


Figure 6. Compressibility effects on heat sink performance

Fig. 6 shows the heat sink's performance with and without air compressibility. The Nusselt number continually increases when

air is treated as incompressible. With the air compressibility is considered, the Nusselt number increases as before and subsequently shows a dip around 80 kHz for  $V_i = 0$  at which the fluid discharge through the orifice is almost ceased. This performance-limiting disruption is seen to shift towards a lower frequency with the introduction of micro passage velocity. However, beyond that frequency, the hybrid heat sink recovers to perform better.

## Conclusions

This study successfully demonstrates the usefulness of a novel thermal enhancement strategy for microchannel heat sinks using a pulsed jet. The proposed synthetic jet with net positive fluid momentum and zero averaged jet mass flow creates excellent thermal characteristics at the impinging heated wall. It delivers up to 120 times heat transfer rates compared to pure natural convection and 4.3 time enhancement compared to pure microchannel heat transfer over the entire frequency range except at a narrow high frequency band where the synthetic jet formation is subdued for fluid compressibility. This hybrid arrangement achieves excellent thermal performance without additional fluid circuits or incurring extra pressure drop, which are recognised as unique attributes of this method that set it apart from other thermal enhancement strategies.

## References

- [1] Lee P.S and Garimella S.V and Liu D. *Investigation of Heat Transfer in Rectangular Microchannels*. Int Journal of Heat and Mass Transfer, 48 (2005), pp. 1688-1704.
- [2] Qu W and Mudawar I. *Experimental and Numerical Study of Pressure Drop and Heat Transfer in a Single Phase Microchannel Heat Sink*. Int Journal of Heat and Mass Transfer, 45 (2002), pp. 2549-2565.
- [3] Lee P.S and Garimella S.V. *Thermally Developing Flow and Heat Transfer in Rectangular Microchannels*. Int Journal of Heat and Mass Transfer, 49 (2006), pp. 3060-3067.
- [4] Fedorov, A.G and Viskanta, R. 2000. "Three Dimensional Conjugate Heat Transfer in the Microchannel Heat Sink for Electronic Packaging". Int Journal of Heat and Mass Transfer, 43(3), pp. 399-415.
- [5] Steinke M.E and Kandlikar S.G. *Single Phase Heat Transfer Enhancement Technique in Microchannel and Minichannel Flows*. Proc of International conference on Microchannel and Minichannels, pp.141-148. ICMM 2004-2328.
- [6] Narayanaswamy R., Chandratilleke T.T and Foong J.L. *Laminar convective heat transfer in a microchannel with internal fins*. Proceedings of the 6<sup>th</sup> International ASME Conference on Nanochannels, Microchannels and Minichannels (ICNMM 2008-62044), Darmstadt, Germany.
- [7] Mahalingam R and Rumigny N. *Thermal Management using synthetic jet ejectors*. IEEE Journal, 27 (2004), pp 439-444.
- [8] Holman R., Utturkar Y., Mittal R., Smith B.L and Cattafesta L. *Formation Criterion for synthetic jets*. AIAA Journal, 43 (2005), pp 2110-2116.
- [9] Smith B.L and Glezer A. *The Formation and evolution of synthetic jets*. Physics of fluids Journal, 10 (1998), pp 2281-2297.
- [10] Chandratilleke T. T., Jagannatha D. and Narayanaswamy R. *Heat transfer enhancement in microchannels with cross-flow synthetic jets*. Int J of Thermal Sc, 49 (2010) pp 504-513.